Independent Primary-Side Controller applied to Wireless Chargers for Electric Vehicles

A. Triviño-Cabrera, M. Ochoa, D. Fernández, J. A. Aguado
Escuela de Ingeniería Industrial
University of Málaga
Málaga, Spain

***Abstract*—Electric vehicles rely on batteries that need to be frequently recharged. As an alternative to conductive charging, wireless chargers provide a higher reliability to pollution and electric failures and they also extend the situations and places where the recharge could be available without user's intervention (e.g. parking spaces, on-road). In order to optimize the performance of a wireless charger, its configuration should be dynamically adapted to the varying battery's electrical features. Towards this goal, controllers are incorporated into the system to modify the behavior of some switching devices belonging to the power electronics blocks. This paper presents a controller that acts in the DC/DC structure placed in the primary side. As a novelty, the controller infers the instantaneous battery power demands by exclusively measuring voltage and current in the primary side. In this way, there is no need for communicating (via wired or wireless links) the primary and the secondary sides. The simulation results show the ability of the controller to adapt to different battery states.**

Keywords— charge, control, electric vehicle, inductively-coupled power system, ICPT, primary-side, SAE J2954

I. INTRODUCTION

Electric vehicles are a reality nowadays. Nissan Leaf, Tesla or Chevrolet Volt are electric vehicles available in the market, and more commercial prototypes will soon appear. In fact, the University of California and Ecotality estimate that the number of PEV (Plug-in Electric Vehicle) will reach 2.5 million in USA by 2020 [1] [2]. However, there still exist several barriers that are restricting their market-expansion. Particularly, current batteries constitute a clear limitation because of their high cost, their short lifetime, the poor autonomy they offer and their excessive recharging time when compared with fuel-based vehicles. Wireless chargers can help overcome the last two shortcomings by allowing a mechanism to extend the possibilities of recharging the vehicle's battery without the user's intervention or even in motion. In this way, we could find wireless chargers in traditional sites such as homes or charging stations but they may also be deployed in some specific public parking spaces or even on the road pavement. For public transport systems like trams or subways, the wireless chargers could be installed in the stops and recharge the batteries while passengers are going up and down the vehicle. Additionally, this kind of chargers avoids the presence, their corresponding impact and the maintenance of the catenaries. This avoidance has become a strong requirement in some historical places. In this sense, Bombardier has developed a tram supported by wireless charger [3].

The core of a wireless charger is constituted by two coupled coils with no physical connection between them. The coils work with VLF (Very-Large Frequency) signals in order to improve the energy transfer from the primary side (coil sited outside the vehicle) to the secondary side (coil installed in the vehicle). Primary side is connected to the electrical network whereas the secondary coil is attached to the battery.

Some power electronics need to be included in the wireless charger to enable the operation at VLF frequencies. Moreover, power electronics also adjust the amount of energy flowing from the electrical source to the battery. This adjustment is a requirement as the battery's features and, in turn, its power demands vary depending on several dynamic parameters such as the temperature or the SOC (State-Of-Charge). In order to tune the transferred power, some control techniques are applied to the power electronics. Basically, the switching times of the power devices are related to the impedance reflected by the battery. As explained in Section II, the control techniques can be performed in the primary side, the secondary side or in both. When measurements from the secondary side are needed by the control system, a link must be established between both parts. Although it could be a wireless link, this kind of control is not robust as both sides become dependent. In this paper, we present a control technique by which an electric vehicle can be charged according to the battery state. The main advantage of the proposal relies on the fact that the controller does not demand any direct information about the battery operation. Indeed, it infers the power needs of the battery from the electrical measurements exclusively performed in the primary side. After this operation, the controller adapts the duty cycle of the DC-DC converter sited in the primary side. This chopper provides the power to the inverter operating at 85 kHz, as it has been recommended by SAE (Society of Automotive Engineers) J2954 [4]. The wireless charger has been designed for trams so it transfers 400 kW to the load in its nominal operation.

The remainder of the paper is structured as follows. Section II reviews some related works about control techniques applied to wireless chargers in electrical vehicles. Section III presents the control technique proposed in this paper. Section IV evaluates the proposal. Finally, Section V draws the main conclusions of our work.

II. Related Work

In the literature, we can find diverse control techniques applied to ICPT (Inductively-Coupled Power Transfer). They could be classified according to the following criteria:

- Localization. It refers to the placement of the controllers, that is, if it is installed in the primary side, the secondary side or in both.
- Magnitudes to adjust. The controller is configured to maintain an electrical magnitude fixed. For instance, it could keep the power, the voltage or the current in the load to a predefined value.
- Power Electronics where it is applied. One or several controller may be present in the ICPT system. In addition, the controllers could act in one or multiple blocks.
- Connection between the primary and the secondary sides. Controllers need some electrical magnitudes as input in order to estimate the state of the system and, in turn, tune some parameters to adjust their output. The input magnitudes could be obtained from a direct connection or derived from a communication system if it has been measured in a side different to the place where the controller is installed. In this last case, controllers can rely on a wired or wireless link to connect both sides.

The proposals in [5] [6] [7] are based on controllers completely installed in the secondary side. [5] [6] act on a DC-DC converter placed previously to the battery. In this way, it aims at delivering a constant voltage to the load. With the same goal, [7] works by altering the secondary compensation structure. [8] also focuses on the load voltage but it adds a controller in the primary inverter to adjust the operational frequency.

Alternatively, the control system proposed in [9] modifies the operational frequency and the input voltage in the inverter with the goal of adjusting the load voltage. This entails some feedback mechanisms to provide the controller of electrical measurements performed in the secondary side. The feedback is avoided in [10], where only measurements from the primary side are considered in order to estimate the load voltage. With this estimation, the inverter is regulated. The main limitation of the work in [10] is that it refers to a LCC compensation topology.

III. Proposed Control Technique

The controller proposed for the primary side of the wireless charger is based on two coupled coils whose features are explained in Subsection A. The structure and the configuration of the ICPT are presented in Subsection B. Then, Subsection C details how to infer the load properties by exclusively measuring in the primary side.

A. Coils design

For its application, we have designed a 400-kW ICPT system, specially intended for trams. As requirements, we have taken into account some of the characteristics of the already implemented tram-ICPT system designed by Bombardier [3]. Precisely, 1000 V and 400 A are delivered to the battery. The most significant difference is that we have set the resonant frequency to 85-kHz in order to follow SAE J-2954 recommendations [4].

In the design process, we have imposed two stability constraints. The first restriction avoids bifurcation. Moreover, the second constraint keeps the system performance constant even when the operational frequency varies 5% of the designed one. Referring to the compensation topology, an SP has been selected due to the benefits reported in [11][12]. This means that a capacitor (C_1) is connected in series in the primary side whereas the capacitor in the secondary side (C_2) is in parallel to the receiver coil.

Table I summarizes the main features of the system.

B. ICPT structure and configuration

The structure of the ICPT system is represented in Figure 1. The ICPT system receives the power from a-three phase electrical network. Then, a non-controlled AC-DC converter is installed providing V_i V to a DC-DC converter. Particularly, a Cûk converter has been selected for this last structure.

TABLE I. ICPT PARAMETERS

Component	Value
L_1 (primary coil inductance)	24.7 μH
L_2 (secondary coil inductance)	1.17 μH
M (mutual inductance)	0.93 μH
Coils geometry	Planar
L_1 dimensions	1 x 0.5 m^2 (4 turns)
L_2 dimensions	0.5x0.5 m^2 (1 turn)
R_1 (resistance offered by the primary coil)	0.45 mΩ
R_2 (resistance offered by the secondary coil)	67.4 $\mu\Omega$
Q_p (quality factor in the primary side)	8.24
Q_s(quality factor in the secondary side)	4.09
C_1 (compensation capacitor in the primary side)	146.3 nF
C_2 (compensation capacitor in the secondary side)	4.09 μF
V_L (load voltage)	1000 V
I_L (load current)	400 A
Power output	400 kW
Nominal efficiency	99.925%
Gap	20 cm
Operational Frequency	85 kHz

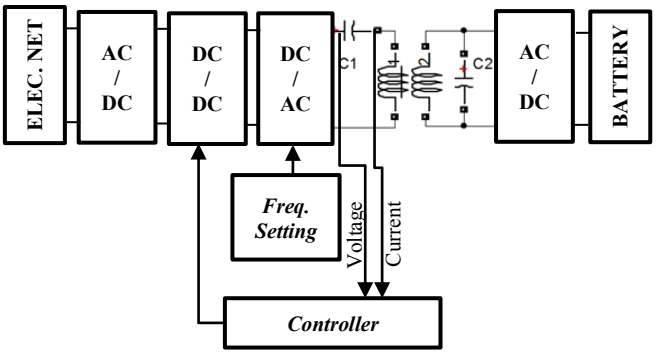

Fig. 1. Structure of the ICPT system

In contrast to a Buck-Boost converter chosen in [9], the Cûk converter is composed of only one switch so its control can be easier. This is an important requirement as the controller acts on the DC-DC switches. Another relevant feature of Cûk converter that led us to select it is that currents traversing coils in a buck-boost converter are higher than those in a Cûk. Thus, coils are cheaper under the selected implementation. Conversely, the Cûk converter requires more components. Specifically, it is supported by two coils (L and L'), two capacitors (C and C'), one switch and a diode. The connection of these elements is shown in Figure 2.

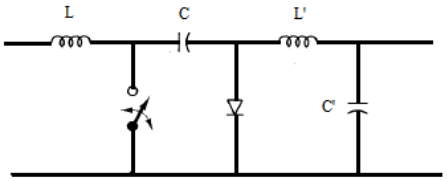

Fig. 2. Electrical scheme of a Cûk converter.

As can be observed, the controller takes the current and the voltage from the primary side as inputs. With this information, a PI controller sets the adequate duty cycle in the DC-DC converter. When the battery is receiving 1000 V and 400 A, that is, 400 kW, the duty cycle is set to 0.626. Precisely, we have experimentally concluded that the output voltage (V_o) and power (P_o) in the Cûk converter must be 910 V and 59.4 kW respectively in order to guarantee the ICPT outputs (voltage and current). Thus,

$$\frac{V_o}{V_i} = \frac{D}{1-D} = \frac{910}{544} \Rightarrow D = 0{,}626 \tag{1}$$

On the other hand, the switching frequency in the DC-DC converter is always kept at 50 kHz. The value of the reactive components in the Cûk converter has been carefully decided. Firstly, the currents traversing the coils (I_L and I'_L) are computed following (2) and (3).

$$I_{L'} = \frac{P_o}{V_o} = 653{,}6\ A \tag{2}$$

$$I_L = \frac{P_o}{V_i} = 1093.75\ A \tag{3}$$

Then, we impose a maximum current ripple of 10% in both elements.

$$L' \geq \frac{V_i D}{f\ \Delta i_{L'}} = 104{,}2\ \mu H \tag{4}$$

$$L \geq \frac{V_i D}{f\ \Delta i_L} = 62{,}27\ \mu H \tag{5}$$

Finally, the values of capacitors C and C' are decided restricting the voltage ripple to 0.5% and 0.1% respectively. In a Cûk converter, this constraint implies that:

$$C' \geq \frac{(1-D)}{\left(\frac{\Delta V_o}{V_o}\right) 8L' f^2} == 17{,}9\ \mu F \tag{6}$$

$$C \geq \frac{V_o D}{R_{eq}\ f\ \Delta V_C} = 97{,}95\ \mu F \tag{7}$$

being R_{eq} the equivalent resistance offered by the converter. In our implementation, the Cûk converter can be modeled as 1.6 Ω.

Alternatively, we can also find an inverter in the primary side. A full-bridge has been configured with square-wave activation signals. Finally, the secondary side includes a non-controller rectifier.

BMS (Battery management system) are usually installed along with the battery to guarantee the correct recharge and, consequently, prolong the battery lifetime. Basically, it allows a constant current or constant voltage on the load depending on the battery state. Taking into account this behavior, our controller based on a PI control has been configured in two different ways: (i) providing a constant voltage in the battery and (ii) ensuring a constant current in the battery. Other configuration approaches are also feasible.

C. Electrical magnitudes inferred in the primary side

The strong requirement imposed on the control system is that it does not rely on a communication from the secondary to the primary side. Thus, it is necessary to infer the battery state and, in turn, its power demand from the electrical measurements performed in the primary side. [10] studies this approach for a LCC compensation topology. As we are opting for a simpler and more robust compensation structure, the aforementioned study cannot be directly applied. Therefore, we derive the relationship between the magnitudes available in the primary side and those required from the secondary side to deduce the battery state when an SP topology is employed. Considering the scheme in Figure 3, we proceed to a circuital analysis. In this model, L_1 is the primary coil, which has an associated resistivity represented by R_1 whereas L_2 is the secondary coil which is linked to a resistor R_2. Additionally, C_1 and C_2 are the compensation capacitors.

Analysing the circuit, we conclude that the current in the load (representing the battery) is as expressed by (8).

$$\bar{I}_2 = \frac{j\omega M}{R_L + R_2 + jR_2R_LC_2\omega + jL_2\omega + j^2L_2C_2\omega^2R_L}\bar{I}_1 \tag{8}$$

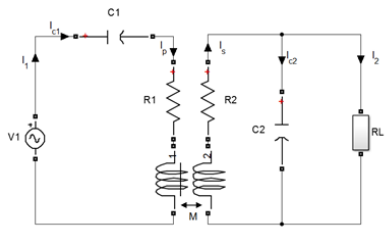

Fig. 3. Simplified electrical scheme of an ICPT system with an SP compensation topology.

Assuming the coils are constructed from good quality material specially intended to work in the VLF range (e.g. Litz wire), R_2 can be neglected in the denominator. As the system is also working in resonance, we state that $L_2C_2\omega^2 = 1$. Thus, (8) is simplified in (9).

$$\bar{I}_2 = \frac{M\bar{I}_1}{R_2R_LC_2 + L_2} \tag{9}$$

Taking into account the battery power demand in the nominal case, we conclude that the secondary impedance reflected in the primary side (Z_r) is:

$$\bar{Z}_r = \frac{\omega^2M^2(1 + jR_LC_2\omega)}{R_L + R_2 + jR_2R_LC_2\omega + jL_2\omega + j^2L_2\omega^2C_2R_L} \tag{10}$$

Neglecting R_2 similarly to [13], we finally obtain:

$$\bar{Z}_r = \frac{M^2R_L}{L_2^2} - j\frac{\omega M^2}{L_2} \tag{11}$$

Thus, the estimated resistance offered by the battery at any instant (R_{Lest}) can be derived as:

$$R_{L_{est}} = \frac{Real\{\bar{Z}_r\} \cdot L_2^2}{M^2} \tag{12}$$

Taking into account the previous analysis, we conclude that it is necessary to simultaneously measure the current ($\bar{I}_1$) and voltage ($\bar{V}_1$) phasors in the primary side to deduce Z_r. Then, the estimated voltage in the battery (V_{Lest}) is approximated as:

$$\bar{V}_{L_{est}} = \frac{R_{L_{est}}M\bar{I}_1}{R_{L_{est}}R_2C_2 + L_2} \tag{13}$$

IV. Simulation Analysis

The evaluation of the proposed technique has been carried out in the Matlab/Simulink tool [14]. We have analyzed the performance of the controller when it has been configured for (i) providing a constant voltage in the load and (ii) ensuring a constant current in the load. In particular, we have set an experiment in which the resistance offered by the battery changes drastically. Firstly, in the interval [0,0.1] s, the battery is working on its nominal working conditions, that is, it is traversed by 400 A and it keeps 1000 V in its connectors. This implies that the battery is modeled as 25 Ω during the first interval. Then, the battery resistance abruptly drops to 50% its initial value during the interval [0.1, 0.2] s. Finally, during the period [0.2, 0.3] s, the resistance increases up to 50 Ω. This setting is not realistic as the battery's resistance tends to vary smoothly. However, the configuration helps evaluating the controller's operation on extreme conditions.

For the first case, when the output voltage is desired to be constant and equal to 1000 V, there exist some transient periods when the battery's conditions are altered. Figures 4 and 5 illustrate the output voltage and current respectively.

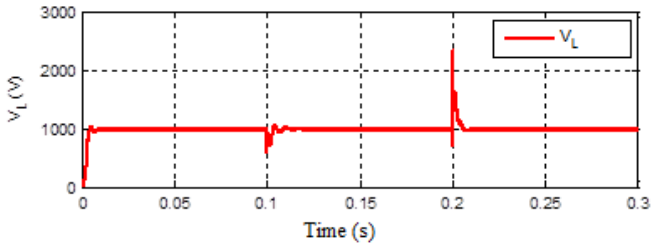

Fig. 4. Voltage in the battery when its resistance is reduced to 50% in the period [0.1,0.2]s and incremented in the period [0.2,0.3]s. A fixed voltage control technique is applied.

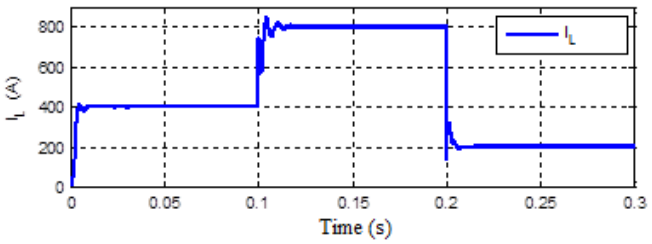

Fig. 5. Current in the battery when its resistance is reduced to 50% in the period [0.1,0.2]s and incremented in the period [0.2,0.3]s. A fixed voltage control technique is applied.

The initial transient time is 0.015 s, which is a much shorter than other controller proposed in the literature such as [15]. The transient time for the first change takes 0.016 s whereas the second transient time lasts 0.006 s. Both figures clearly demonstrate the goodness of the controller as it is able to provide a constant voltage at the load. In fact, we have verified that the estimated voltage is exactly the same as the output voltage. This coincidence is represented in Figure 6. Nevertheless, keeping the output voltage constant implies that the output power is modified. Precisely, this magnitude ranges from 400 kW in the nominal operation state to 800 kW in the second interval and to 200 kW in the last period. When an electric design is based on reactive components, a key issue is the maximum voltage and currents they have to support. For the capacitors belonging to the compensation topologies, the abrupt changes has led to a maximum value of 12750 V in C_1. The voltage in C_2 is always 1000 V as it is placed in parallel with the load.

The second configuration tested obliges current in the load to be kept constant, independently of the battery features. We have also evaluated the controller on the extreme previous setting with abrupt variations of the battery resistance. Under these circumstances, the controller behaves as represented in Figures 7 and 8. Once again, the controller is able to provide the constant magnitude as demanded. As can be observed, the transient times are not relevant.

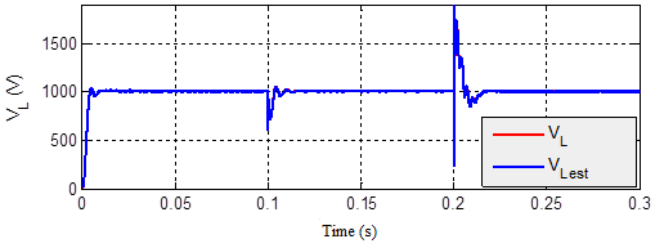

Fig. 6. Estimated output voltage versus measured output voltage in the ICPT system.

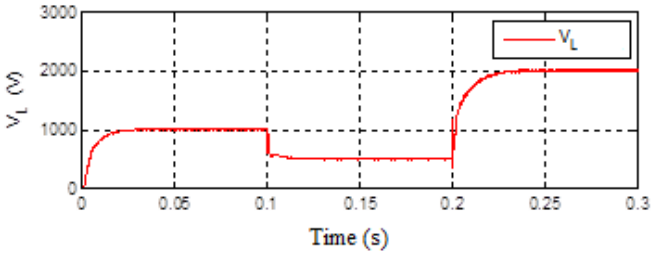

Fig. 7. Voltage in the battery when its resistance is reduced to 50% in the period [0.1,0.2]s and incremented in the period [0.2,0.3]s. A fixed current control technique is applied.

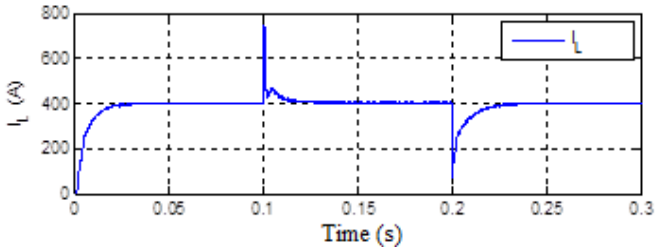

Fig. 8. Current in the battery when its resistance is reduced to 50% in the period [0.1,0.2]s and incremented in the period [0.2,0.3]s. A fixed current control technique is applied.

V. Conclusions

This paper presents a controller that adapts the configuration parameters of a wireless charger in order to maintain a constant magnitude in the electric vehicle's battery independently on its state. The most relevant feature of the designed controller relies on the fact that it is not support by any kind of communication system from the primary side to the secondary. Due to this restriction, the controller must infer the status of the battery from the measurements available in the primary side. An analytical relationship to estimate battery's voltage from the current and voltage in the primary side has been derived in the paper. This expression has been obtained for an ICPT system with an SP compensation topology.

The simulation results show the ability of the controller to keep current or voltage (depending on the selected configuration) constant in the load. The evaluation has been carried out in an experiment where the resistance offered by the battery dramatically changes.

As a future work, we intend to extend the controller in order to regulate two magnitudes simultaneously: the voltage/current delivered to the load and the power factor perceived by the electrical network.

The extended version of the paper will include an analysis about the magnitudes supported by the switching devices in the complete ICPT system.

Acknowledgment

This work has been partially funded by Universidad de Málaga, Campus de Excelencia Internacional Andalucia Tech.

References

[1] T.A. Becker, I. Sidhu, B. Tenderich, " Electric Vehicles in the United States: A New Model with Forecasts to 2030", University of California, Berkley, August 2009.

[2] ECOtality North America. "Long-Range EV Charging Infrastructure Plan for Western Oregon", August 2010.

[3] Primove light rail. Bombardier. Avaiable, August 2014.

[4] SAE international task force announces agreement on frequency of operation and power classes for wireless power transfer for its electric and plug-in electric vehicle guideline, August 2014.

[5] N. A. Keeling, J. T. Boys, G. A. Covic, "A unity-power-factor IPT pickup for high-power applications", IEEE Transactions on Ind. Electron., vol. 57, issue: 2, pp 744-751. Feb. 2010.

[6] G. Elliott, S. Raabe, J. T. Boys, G. A. Covic, "Multiphase pickups for large lateral tolerance contactless power-transfer systems", IEEE Transactions on Industrial Electronics, vol. 57, issue: 5, pp 1590-1598. May. 2010.

[7] J-U W. Hsu, A. Swain, A. P. Hu, "Implicit Adaptive Controller for Wireless Power Pick-ups", Proc on IEEE Conference on Industrial Electronics and Applications, pp. 514-519. June 2011.

[8] J. Yungtaek, M. Jovanovic, "A Contactless Electrical Energy Transmission System for Portable-Telephone Battery Chargers", IEEE Transactions on Ind. Electron., vol 50, issue: 3, pp 520-527. June 2003.

[9] L-R Chen, H-W Chang, C-H Wu, C-M Young, N-Y Chu, "Voltage Controllable Power Factor Corrector based Inductive Coupling Power Transfer System", Proc. on IEEE Conference on Industrial Electronics, pp. 582-587, May 2012.

[10] U.K. Madawala, D. J. Thrimawithana, "New technique for inductive power transfer using a single controller", IET Power Electronics, vol. 5, issue: 2, pp 248-256. Feb. 2012.

[11] Y. Chao, J. Shieh, C. Pai, W. Shen, "A closed-form oriented compensator analysis for series-parallel loosely coupled inductive power transfer systems", Proc. IEEE Power Electronics Specialists Conference, (PESC 2007) , pp. 1215-1220, 2007.

[12] W. Zhou, H. Ma, H, "Design Considerations of compensation topologies in ICPT system", Proc. IEEE Conference on Applied Power Electronics (APEC 2007) , pp. 985-990, 2007.

[13] C-S Wang, G.A. Covic, O.H. Stielau. "General Stability Criterions for Zero Phase Controlled Loosely Coupled Inductive Power Transfer Systems", Proc. IEEE Conference on Industrial Electronics Society, vol. 2, pp. 1049-1054. Nov. 2001.

[14] Mathworks, August 2014.

[15] S. Selvaperumal, C.C.A. Rajan, "Investigation of closed-loop performance for an LCL resonant converter in a real-time operating system environment". IET Power Electronics, vol. 5, issue: 5, pp. 511-523. May. 2012.